Tetrahedron 66 (2010) 7605–7611

Contents lists available at ScienceDirect

Tetrahedron

journal homepage: www.elsevier.com/locate/tet

Novel method for the synthesis of functionalized tetrathiafulvalenes, an acceptor–donor–acceptor molecule comprising of two *o*-quinone moieties linked by a TTF bridge

Viacheslav Kuropatov [a,*], Svetlana Klementieva [a], Georgy Fukin [a], Aleksander Mitin [a], Sergey Ketkov [a], Yulia Budnikova [b], Vladimir Cherkasov [a], Gleb Abakumov [a]

[a] G.A. Razuvaev Institute of Organometallic Chemistry of Russian Academy of Sciences, Tropinina str., 49, 603950, Nizhny Novgorod, Russian Federation
[b] A.E. Arbuzov Institute of Organic and Physical Chemistry of Russian Academy of Sciences, Arbuzov str. 8, Kazan, 420088 Russian Federation

ARTICLE INFO

Article history:
Received 1 April 2010
Received in revised form 24 June 2010
Accepted 15 July 2010
Available online 22 July 2010

Keywords:
o-Quinone
Tetrathiafulvalene
Tetrathiooxalate
Acceptor–donor–acceptor triad

ABSTRACT

In search of a synthesis of *o*-quinone-tetrathiafulvalene-*o*-quinone triads a novel facile route was developed. Sodium tetrathiooxalate was for the first time used as a synthon in functionalized TTF preparation. The main purpose of this work was to construct an organic compound, which on the one hand possesses a redox-amphotericity, and on the other hand can act as a bridging ligand in construction of linear, 2D and 3D assemblies. Properties of new acceptor–donor–acceptor ligand in respect to application as a building block for the molecular devices have been investigated.

1. Introduction

During the last few years, there has been increasing interest in the search for organic compounds exhibiting a low HOMO–LUMO gap[1] due to their potential application in molecular electronics and optoelectronics. A possible way to achieve this aim is a combination of covalently linked donor and acceptor moieties in one molecule.[2] TTF is widely used as an acceptor in the construction of such systems.[3] Here we present the preparation of such A–D–A system consisting of two sterically hindered *o*-quinone moieties connected via fused TTF bridge. An analogous molecule containing *p*-quinone **1** instead of *o*-quinone have been studied by Hudhomme et al.[4,5] (Fig. 1).

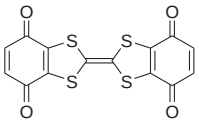

1

Figure 1. *p*-Quinone–TTF–*p*-quinone triad (**1**).

o-Quinone is a stronger acceptor as compared with *p*-quinone, in addition it can act as a chelating ligand to form stable complexes with various transition and non-transition metals. Moreover, transition metals in such complexes can change their oxidation state when the metal environment is altered.[6–8] In turn, these properties suggest that the use of these species as building blocks in the construction of 2D and 3D assemblies may lead to molecular wires, and perhaps even molecular rectifiers. So, our main purpose was to synthesize redox-amphoteric, planar, rigid, fully conjugated, and bridging ligands with the non-Kekulé structure. A molecule combining redox-amphotericity and ability to act as a ligand is reported for the first time in this work.

There are several synthetic approaches to TTF.[2,9] Most of these synthetic procedures for preparation of symmetrically functionalized TTF proceed with a key intermediate, which already contains the 1,3-dithiol ring. The final stage is homocoupling of 1,3-dithiol-2-one or corresponding thione using phosphines or phosphites. This method includes a prior protection of all other carbonyl and hydroxyl groups before the dimerization, followed by deprotection procedures.

In this work fused triad, *o*-quinone–TTF–*o*-quinone, was prepared via a novel synthetic route. In contrast to strategies previously used for TTF syntheses, our method does not require complicated and prolonged procedures of protection/deprotection of carbonyl groups. Moreover, all processes can be conducted

* Corresponding author. Tel.: +7 831 462 7682; fax: +7 831 462 7497; e-mail address: viach@iomc.ras.ru (V. Kuropatov).

0040-4020/$ – see front matter © 2010 Elsevier Ltd. All rights reserved.
doi:10.1016/j.tet.2010.07.038

sequentially in one-pot. It seems to us that the analogous route could be extended for the incorporation of the TTF functionality between two aromatic fragments.

2. Results and discussion

At the beginning of the work we chose the classic synthetic strategy toward the preparation of the conjugated *o*-quinone–TTF–*o*-quinone system. According to this concept we considered the quinone **2** as the starting material for the preparation of a target product. Despite many efforts associated with variation of experimental conditions the dimerization products in the resulting crude mixture were not observed. Moreover, treatment of quinone **2** with excess triethylphosphite results only in formation of dioxaphospholane species **3**. It is rather surprising that the carbonyl group in the five-membered ring remains unchanged in this reaction (Scheme 1).

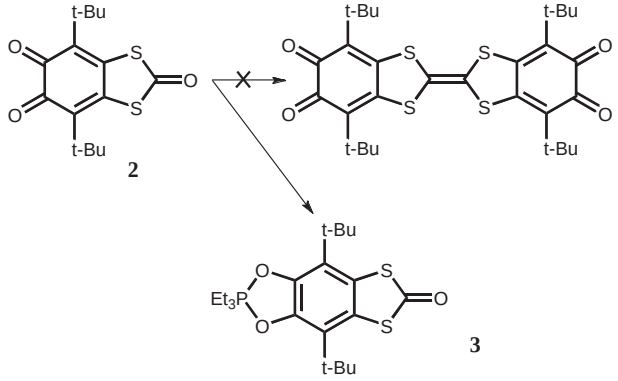

Scheme 1. Homocoupling of **2**: $(EtO)_3P$, THF, 2 h, 60 °C.

A novel strategy, which allows incorporation of the TTF group in conjugated and extended A–D–A systems, has been developed. This strategy gives the opportunity to obtain the desired species in a good yield. The main idea was to assemble the fused A–D–A system directly in the course of the template synthesis. 4-Chloro-3,6-di-*tert*-butyl-*o*-benzoquinone **4** (2 equiv) were combined with 1 equiv of sodium tetrathiooxalate Na_2(tto), which already contains the $S_2C–CS_2$ motif. It should be noted that this is the first usage of a tetrathiooxalate salt as a precursor for TTF syntheses.

Sodium tetrathiooxalate Na_2(tto) have been synthesized starting from elemental sodium and sulfur according to the method proposed by Takata et al.[10,11] (Scheme 2) In order to manipulate a gram scale of anhydrous Na_2S_2 we optimized the synthetic procedure and exploited an ultrasonic bath. The interaction between sodium and sulfur was conducted in a degassed glass ampoule at 80 °C in dimethoxyethane in the presence of catalytic amounts of benzophenone. Then Na_2S_2 was treated with tetrachloroethylene to give Na_2(tto) according to the method described by Breitzer et al.[12] The anion tto^{2-} is very labile and tends to transform into $C_4S_6^{2-}$ in solution.[12] This makes isolation and storage of Na_2(tto) inexpedient. Thus, Na_2(tto) should be used instantly after preparation. A solution of Na_2(tto) in methanol/MeCN was gradually added to 2 equiv of quinone **4** dissolved in MeCN under vigorous stirring. The reaction proceeds instantly on mixing the reactants (Scheme 3). The color of the solution of quinone turns from red to deep blue. Intermediate product **5** was not isolated because subsequent cyclization into five-membered ring occurs simultaneously. We propose that the mechanism of this reaction is similar to that reported previously for the reaction of **4** with sodium xanthate.[13] Quinone-catechol **6** was then oxidized with alkaline potassium ferricyanide to give bis-quinone **7**. Bis-*o*-quinone **7** was isolated as dark violet prismatic crystals with a yellowish metallic luster.

According with the TLC data, the conversion of **4** in this reaction is close to 100%. Bis-*o*-quinone **8**, containing sulfur bridge was obtained as the only byproduct together with the main product **7**.

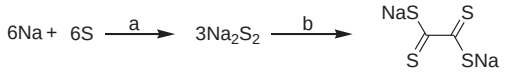

Scheme 2. Preparation of sodium tetrathiooxalate: (a) DME, 80 °C, ultrasonic bath, 50 h; (b) tetrachloroethylene, MeOH/MeCN, 5 min.

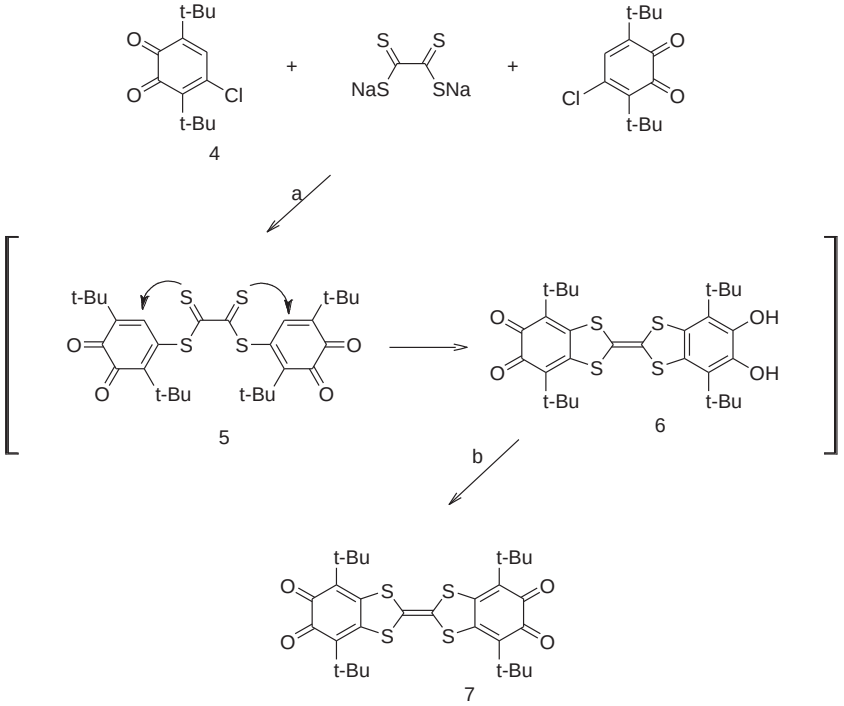

Scheme 3. Preparation of **7**: (a) MeOH/MeCN solution, 5 min, rt, −NaCl; (b) ether/H_2O, $K_4[Fe(CN)_6]$, K_2CO_3, rt, 10 min.

Crude mixture consists of two quinones **7** and **8** in the ratio 3:2, which were separated from each other by crystallization. Formation of **8** can be attributed to the admixture of Na_2S in the parent disulfide. To prove this hypothesis we conducted the reaction of Na_2S with **4**. Quinone **8** was obtained in a quantitative yield. Its structure was established by X-ray analysis. Compound **8** was isolated as octahedron-shaped dark-brown crystals. Its physical and chemical properties are very much alike with those of other sterically hindered *o*-quinones.[14–16] Thus, it can be reduced with alkali metals and thallium to give corresponding semiquinone complexes. All additional information on this compound can be found in the Supplementary data (Fig. 2).

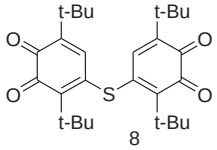

Figure 2. Bis-*o*-quinone (**8**).

Compound **7** is stable to air in the solid state and in solution, but it is relatively photosensitive. Its diluted solutions lose color when being exposed to visible light over 5–7 h. Crystals of **7** grown from methylene chloride lose the lattice solvent and crumble on air. Its decomposition starts near the melting point at 243 °C. All the spectroscopic data (^{1}H and ^{13}C NMR, IR) for **7** are in agreement with the proposed structure. The IR spectrum shows a well pronounced downward shift of the carbonyl stretching (1647, 1629 cm^{-1}) with respect to the corresponding values of 3,6-di-*tert*-butyl-*o*-benzoquinone (1679, 1656 cm^{-1}).[17] This behavior is explained by the partial charge transfer from TTF fragment toward the quinone moieties. In $CDCl_3$ the ^{13}C NMR spectrum of **7** consists of a peak at δ 117.2 ppm, which is characteristic for the C=C atoms in the TTF functionality.[18–20]

Due to the bulky hydrophobic *tert*-butyl substituents, compound **7** is readily soluble in most polar organic solvents such as THF, chloroform, dichloromethane, DME or acetone and moderate soluble in saturated hydrocarbons.

The combination of a strong donor (TTF) and a weak acceptor (*o*-quinone) in one molecule results in a facile intramolecular electron transfer, which is manifested in an intense band in the 370–650 nm region in the electronic absorption spectrum of **7**. The maxima of absorption is strongly dependent on the solvent used (e.g., λ_{max}=564 nm, ε=31,000 M^{-1} cm^{-1} in CH_2Cl_2) (Fig. 3). Extremely high extinction values have been observed in all the solvents used. As a rule, a state with a partial charge transfer is stabilized in polar solvents, which is manifested in a red-shift of absorption band (Table 1). Very similar behavior was reported for the *p*-quinone A–D–A analogue[4,5] **1**, but the observed CT band of **7** is blue-shifted and the absorption coefficient is almost 40 times as large as those of **1**.

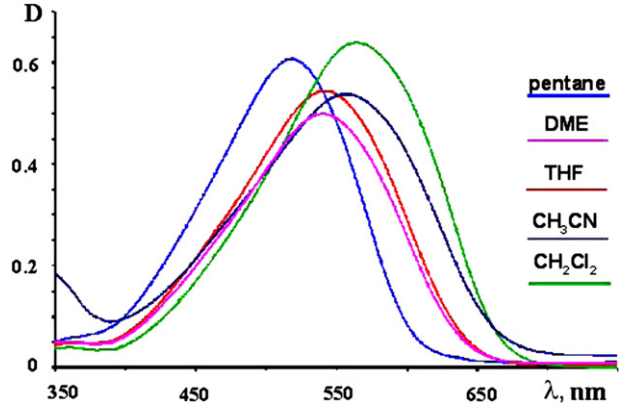

Figure 3. Solvatochromic shift of absorption maxima of **7** in different solvents.

Table 1
Wave lengths and extinction molar coefficients of absorption maxima of **7** in different solvents

Solvent	E_T^N[a]	λ_{max} (nm)	$\varepsilon\times10^{-4}$ (M^{-1} cm^{-1})[b]
Pentane	0.009	518	3.04±0.04
Et_2O	0.117	527	3.17±0.09
THF	0.207	539	2.70±0.03
DME	0.231	542	2.53±0.05
CH_3CN	0.460	556	2.69±0.04

[a] E_T^N—empirical parameter of solvent polarity.[21]
[b] Extinction ε was measured in the concentration range from 3×10^{-5} to 3×10^{-4} M.

In cyclic voltammetry (CV) experiments, **7** showed reduction behavior consisting of four single-electron waves at −0.40, −0.61, −1.04, and −2.56 V (E_{red}, DMF, vs Hg/Hg_2Cl_2) (Fig. 4). Two first waves are fully reversible, the other two waves are quasi reversible. Oxidation in DMF occurs at E_{ox}=1.40 V and is irreversible (Fig. 5). Such behavior can be explained by a partial oxidation of the solvent, which can take place at this potential.

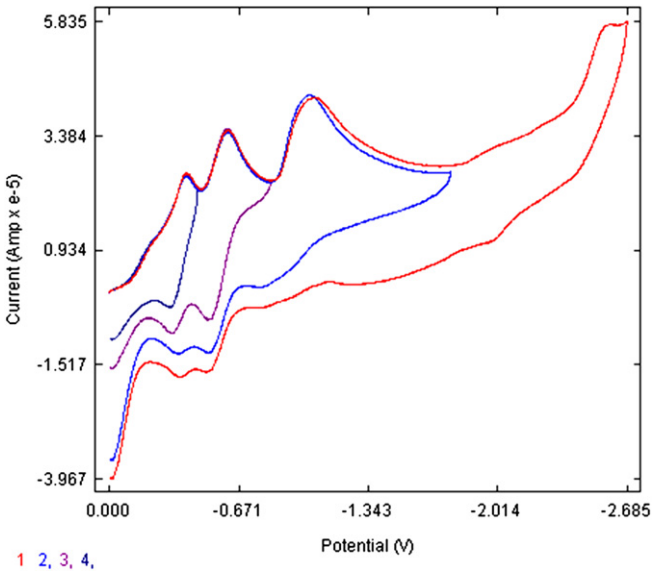

Figure 4. Cyclic voltammogram of **7** (5×10^{-3} M) in DMF (reduction).

Cyclic voltammograms were also recorded in *p*-dichlorobenzene/MeCN mixture. There are three reduction waves at −0.48, −0.72 and −1.22 V (E_{red}, vs Hg/Hg_2Cl_2) and two oxidation waves at 1.62 and 1.82 V (E_{ox}) (see Supplementary data). The first and the second reductions are one-electron and these are reversible. The third reduction wave and both oxidations in *o*-dichlorobenzene/MeCN mixture are irreversible. Compound **7** is poorly soluble in solvents, which are usually employed in electrochemical experiments. It is difficult to find a solvent providing both a good solubility for the titled compound and a high resistance to oxidation. Nevertheless, the presence of four distinct reduction waves in CV recorded in DMF shows that two quinone moieties effectively interact via the TTF bridge. The extremely high value of the oxidation potential is not characteristic for tetrathiafulvalenes. All the TTF derivatives are oxidized in the range 0.32–0.80 V[2] ($E_{½}$), i.e., unsubstituted TTF has a first half-wave oxidation potential of 0.34 V.[22] A remarkably large anodic shift, observed for the TTF oxidation wave in **7**, is ascribed to the strong electron-withdrawing effect of the fused *o*-quinone moieties.

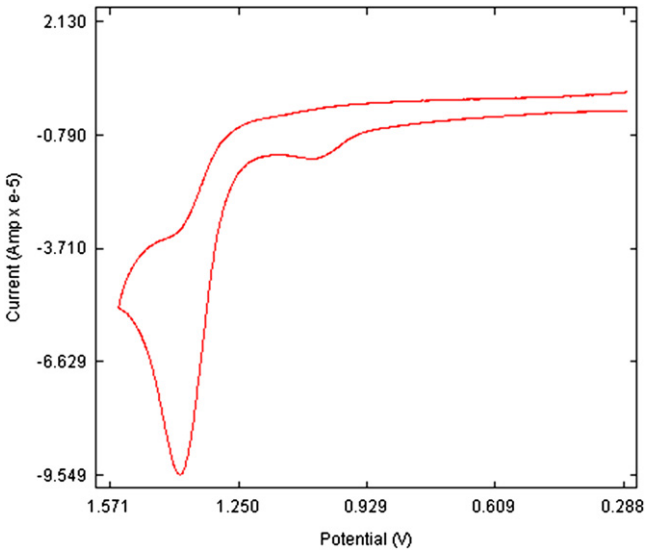

Figure 5. Cyclic voltammogram of **7** (5×10^{-3} M) in DMF (oxidation).

Like many sterically hindered *o*-quinones, compound **7** can be easily reduced in solution with alkali metal or thallium amalgam. Reduction proceeds stepwise to give mono-, di-, tri, and tetraanionic species, respectively. The color of the solution converts from violet to deep blue and then to brownish-green. Tri- and tetraanions of **7** are almost insoluble. EPR monitoring of the reduction of **7** with sodium in THF shows formation of a semiquinone radical-anionic species at the first stage (Fig. 6a). The spectrum is centered at g=2.0047, the quartet splitting is due to the coupling of the electronic spin with the sodium nucleus (a_{Na}=0.40 G). The spectrum lines are rather narrow with the HFS constant value on metal being typical for sodium complexes with symmetrical sterically hindered *o*-quinones.[23] Further reduction of monosemiquinone leads to the appearance of another quartet signal in the EPR spectrum. This signal is observed at the same time with the monosemiquinone quartet and is centered at g=2.0050 and reveals the HFS constant on sodium (a_{Na}=0.37 G, Fig. 6b). The intensity of the first quartet decreases up to full disappearance with simultaneous growth of the second one (Fig. 6c). We suppose that the second signal indicates the formation of a triply reduced derivative of **7**. A doubly reduced binuclear complex seems to be EPR silent. Its diamagnetism could be explained by the effective coupling of unpaired electrons situated on the semiquinone termini via the conducting TTF bridge. Exhaustive reduction of **7** results in formation of an insoluble tetranuclear sodium complex. This powder exhibits a weak EPR signal, but taking into account its intensity, it can be attributed to the admixture of paramagnetic trinuclear species. Notably, addition of equivalent amounts of **7** to the tetranuclear complex results in formation of mono-, di-, and trireduced adducts, respectively.

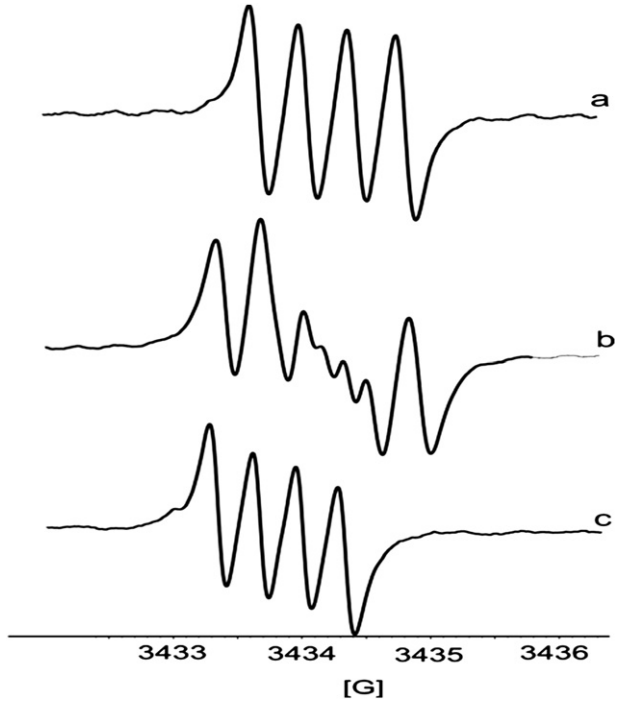

Figure 6. Evolution of the EPR spectra of **7** upon reduction with sodium in THF.

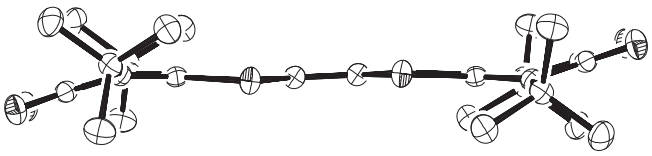

Figure 7. A side view of **7a**.

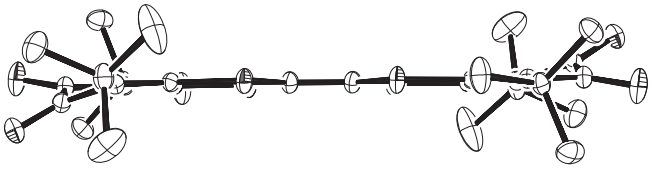

Figure 8. A side view of **7b**.

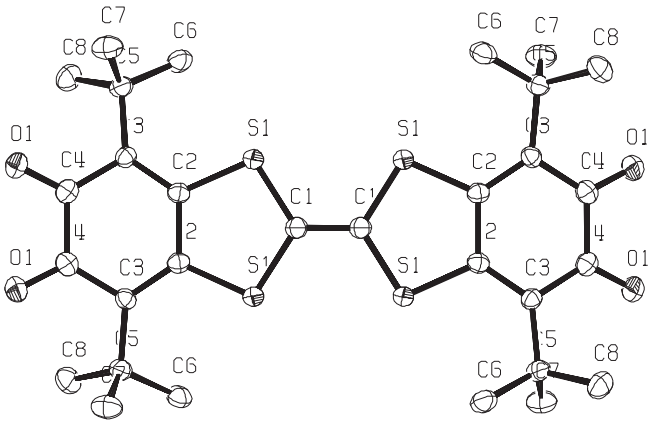

Figure 9. A front view of **7a**.

Two polymorph samples of **7** were studied by X-ray crystallography. The first one was grown by slow cooling of a concentrated solution of **7** in dichloromethane/hexane (**7a**), the second one was obtained from an acetone/hexane mixture (**7b**). Both **7a** and **7b** contain dichloromethane and acetone in their crystal lattices, respectively. Molecules of **7a** are packed in stacks so that the TTF planes are parallel to each other (Fig. 10). The generatrix of the stack is normal to the planes of the molecules. Moreover the carbonyl groups of the adjacent molecules in a stack are situated directly above the sulfur atoms of the TTF moiety. The intermolecular distance between the face-to-face planes of the adjacent molecules

(d=3.66 Å) shows a significant overlap comparable with the plane-to-plane distances between donor and acceptor molecules in crystals of mixed-stack intermolecular charge transfer complexes. The shortest intermolecular atom–atom distance of 3.22 Å in **7a** is observed between the atom O1 of one molecule and the atom S5 of the adjacent molecule. The intermolecular contacts can be attributed to the dipole–dipole interaction between the electron-poor atom O1 and the electron-rich atom S5 (Fig. 9).

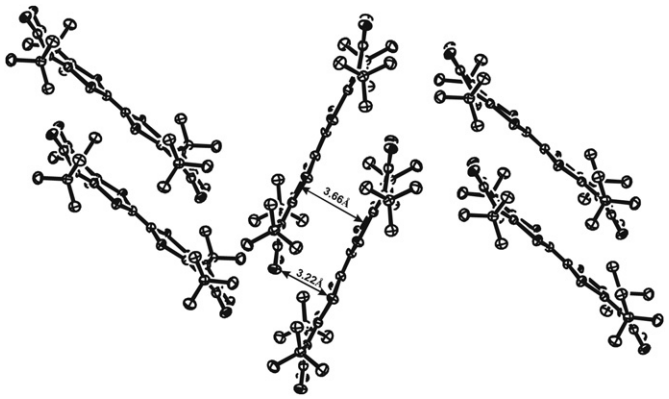

Figure 10. A crystal structure of **7a**.

The crystal lattice of **7b** consists of molecules that are built in interpenetrating stacks (Fig. 11). The shortest intermolecular distance in one stack is 8.80 Å but each quinone moiety is placed above a TTF moiety of a molecule from an adjacent stack, with the distance between the quinone carbonyl and sulfur atom being 3.32 Å, which is close to the sum of the Van der Waals radii.

The central C–C bonds of the TTF moiety in both polymorphs **7a** and **7b** are longer than the standard double bond (1.34 Å).[18–20] This fact might be ascribed to the contribution of a dipolar structure to the ground state. An estimated value of CT derived from the structural parameters according to method proposed earlier[18] is 0.3 for **7a** and 0.1 for **7b**.

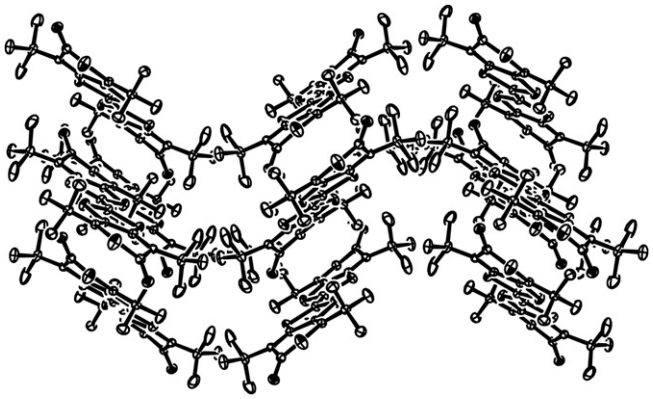

Figure 11. A crystal structure of **7b**.

X-ray crystallography revealed that the molecules of **7a** and **7b** are nearly planar. The difference between **7a** and **7b** is due to distortion of the quinone rings. The distortion is caused by the steric repulsion between *tert*-butyl substituents both from the sulfur and oxygen atoms. This repulsion forces the quinone ring in **7a** to skew along the axis of *tert*-butyl substituents, so that carbonyl groups are bent in the same dimension from the molecule ring (Fig. 7). The carbonyl groups of the second quinone ring are bent in the opposite direction. Another distortion is observed in the case of **7b**. To reduce the steric repulsion from the *tert*-butyl substituents, the carbonyl groups of one quinone ring protrude in the opposite direction from the molecular plane (Fig. 8).

Density Functional Theory (DFT) calculations of the fused A–D–A system were performed using Gaussian 03 at the B3LYP/6-31G* level of theory for a full geometry optimization, with no symmetry constraints. Even if no symmetry was imposed, the optimized geometry obtained was close to the D_{2h} point group. The optimized structure is very similar to that observed experimentally in **7b**, the carbonyls from one quinone ring are bent in the opposite dimensions from the plane of the molecule. Calculations of **7** show that the LUMO is delocalized primarily over the quinone rings and the oxygen atoms, and the HOMO belongs to the $S_2C{=}CS_2$ framework (Figs. 12 and 13). The calculated energies for HOMO and LUMO are −5.81 eV and −3.39 eV, respectively. The HOMO–LUMO gap in **7** was estimated to be 2.41 eV. This indicates that the absorption band at 514 nm (2.41 eV) can be assigned to the intramolecular charge-transfer transition HOMO→LUMO. Commonly, *o*-quinones are the better acceptors compared with the analogous *p*-quinones. Taking this into account we expected the HOMO–LUMO gap in **7** to be smaller than value 1.46 eV observed by Dumur et al. for **1**.[4] To understand this fact we compared the contribution from the TTF fragments to HOMO for **7** and **1**. These values are 74% and 87%, respectively. A relatively high contribution of quinone orbitals in HOMO increases the HOMO–LUMO gap value for **7**. These data are in a good agreement with high oxidation potential determined by CV experiments.

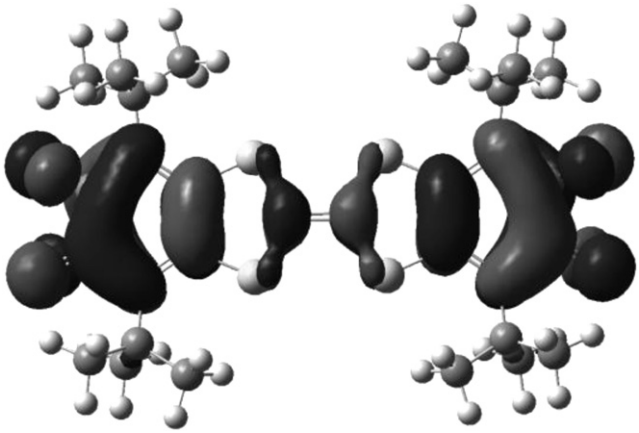

Figure 12. LUMO orbital of **7** obtained by DFT calculations.

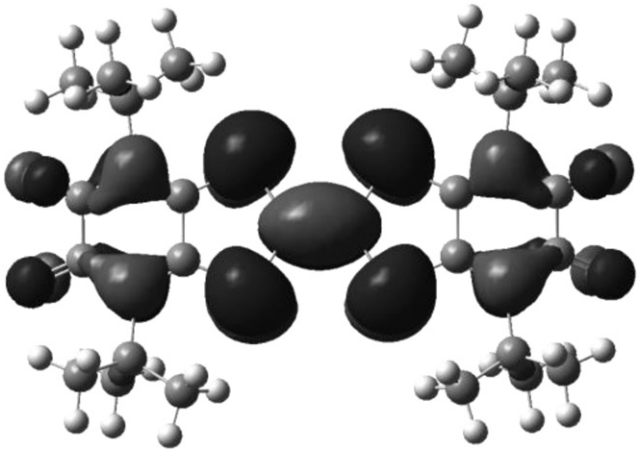

Figure 13. HOMO orbital of **7** obtained by DFT calculations.

Thus, results of X-ray investigations, electrochemical data as well as DFT calculations show that the donor ability of the TTF moiety in **7** is essentially weakened compared with the non-substituted tetrathiafulvalene. At the same time, the *o*-quinone function, which is presumably determined by the energy of LUMO seems to be only slightly disturbed by an annealed TTF fragment.

3. Conclusion

We have developed a novel synthetic route for the preparation of functionalized tetrathiafulvalenes. Also we have synthesized the first *o*-quinone–TTF–*o*-quinone acceptor–donor–acceptor triad. The presence of both electron donor and acceptor fragments results in a multistage amphoteric redox behavior. The HOMO–LUMO gap for compound **7** is estimated from DFT calculations to be 2.41 eV. Proposed strong charge transfer in compound **7** agrees with an intense CT band in the electronic absorption spectrum, which can be assigned as the HOMO→LUMO transition.

4. Experimental section

4.1. General procedures

IR spectra were recorded on a FSM-1201 FTIR spectrometer in Nujol. UV/vis spectra were measured on a Perkin–Elmer Lambda 25 spectrometer in 0.1 cm quartz cells. CV experiments were carried out using an E2P Epsilon potentiostat equipped with a three-electrode cell C3. The scan rate is 100 mV/s. ^{1}H and ^{13}C NMR spectra were obtained on a Bruker Avance III 400 MHz and Bruker DPX 200 MHz instrument. The chemical shifts are expressed in parts per million downfield relative to internal tetramethylsilane (δ=0 ppm) or chloroform (δ=7.26 ppm). X-band EPR spectra were recorded with Bruker a EMX spectrometer. The samples for EPR study were prepared according to procedures described by Prokof'ev et al.[23] Elemental analyses were carried out with a EURO EA machine. X-ray analysis was carried out on a Bruker Smart Apex diffractometer. Polyethyleneterephthalate sheets covered by the homogeneous silica gel sorbent layer Sorbfil-TLC-P were used for TLC analyses. Solvents were purified and dried by standard procedures.[24] Tetrachloroethylene (CAS №° 127–18-4) was used as received from Aldrich Chemical Co. Unless noted otherwise, synthetic procedures were carried out under vacuum.

4-Chloro-3,6-di-*tert*-butyl-*o*-benzoquinone was synthesized as described by Garnov et al.[25] starting from 3,6-di-*tert*-butyl-*o*-benzoquinone, which was prepared according to a known procedure.[17]

4.1.1. Disodium disulfide. Sodium (1.15 g, 50 mmol) was melted in dry diglyme, washed from alkali and dried in vacuum. Then sulfur powder (1.61 g, 50 mmol) and a solution of benzophenone (0.11 g, 0.6 mmol) in DME (40 mL) were added. The reaction mixture was sealed and then treated for 50 h at 80 °C in an ultrasonic bath until the sodium completely disappeared.

4.1.2. Disodium tetrathiooxalate. An ampoule of Na_2S_2 suspension in DME was opened and the solvent was removed in vacuum. The residue was dissolved in MeOH (10 mL) and diluted with CH_3CN (50 mL). Then the mixture was filtered to remove unreacted sulfur to give an orange-brown solution. A tenfold excess of tetrachloroethylene (8.5 mL, 83 mmol) was added to this solution and the mixture heated for 5 min at 80 °C in a water bath. The color of the solution changed to dark-brown and sodium chloride precipitated. Once prepared the solution of Na_2(tto) was immediately used in the following synthesis without purification.

*4.1.3. 4,4′,7,7′-Tetra-tert-butyl-2,2′-bi-1,3-benzodithiole-5,5′,6,6′-tetrone (**7**).* A solution of Na_2(tto) was added to 4-chloro-3,6-di-*tert*-butyl-*o*-benzoquinone (4.32 g, 17 mmol) dissolved in CH_3CN (10 mL) at rt. A color of the mixture turned to deep-blue. The solvent was removed in vacuum and the residue was gradually extracted with Et_2O (500 mL). The ethereal solution was oxidized on air with a large excess of alkaline potassium ferricyanide solution. The completeness of the oxidation was checked by TLC. The ether layer was washed with water and evaporated. The residue was washed repeatedly with small portions of hexane to remove 4,4′-thiobis(3,6-di-*tert*-butylcyclohexa-3,5-diene-1,2-dione). Di-*o*-quinone **7** was isolated (1.22 g, 25%) as violet crystals with yellowish metallic luster after crystallization at −18 °C from CH_2Cl_2/hexane. Mp: 243 °C. A sample suitable for crystallography was obtained after recrystallization from the mixture CH_2Cl_2/hexane (1/10) and acetone/hexane (1/5). Anal. Calcd (%) for $C_{30}H_{36}O_4S_4$ (588.86 g mol^{-1}): C 61.19, H 6.16, S 21.79; found: C 60.97, H 6.19, S 21.90; IR: ν=1647, 1629, 1496, 1478, 1393, 1363, 1294, 1218, 1091, 1025, 995, 913w, 840, 816, 765, 641, 538, 463 cm^{-1}; ^{1}H NMR (200 MHz, $CDCl_3$, 25 °C, TMS): δ=1.47 ppm (s, 36H; 4^{t}Bu); ^{13}C NMR (50 MHz, $CDCl_3$, 25 °C, TMS): δ=29.9 (C(CH_3)$_3$), 37.5 (*C*(CH_3)$_3$), 117.2 (C=C of TTF core), 140.1, 149.3 (C=C of *o*-benzoquinone rings), 183.3 ppm (C=O).

*4.1.4. 4,4′-Sulfanediylbis(3,6-di-tert-butylcyclohexa-3,5-diene-1,2-dione) (**8**).* Compound was extracted with hexane from a crude product formed in the previous reaction. Solvent was evaporated. Octahedron-shaped dark-brown crystals were isolated from acetone (1.55 g, 39%). Mp 201–202 °C. Anal. Calcd (%) for $C_{28}H_{38}O_4S$ (470.64 g mol^{-1}): C 71.45, H 8.14, S 6.81; found: C 71.31, H 8.07, S 6.77; IR: ν=1671s, 1653s, 1611m, 1535w, 1517m, 1481m, 1360m, 1279m, 1260s, 1212s, 1158s, 1028w, 952m, 931w, 898m, 837m, 795w, 756m, 720w, 647w, 580w, 508w cm^{-1}; ^{1}H NMR (200 MHz, $CDCl_3$, 25 °C, TMS): δ=1.16, 1.48 (both s, both 18H; 2^{t}Bu), 6.64 ppm (s, 2H); ^{13}C NMR (50 MHz, $CDCl_3$, 25 °C, TMS): δ=28.8, 30.6 (2C(CH_3)$_3$, 2C′($C'H_3$)$_3$), 35.2, 37.4 (2*C*(CH_3)$_3$, 2*C*′($C'H_3$)$_3$), 138.9, 142.0, 148.3, 153.2 (C=C, C′=C′), 182.7, 184.1 (2C=O, 2C′=O).

4.2. X-ray crystallographic study

Diffraction data for **7** and **8** were collected at 100 K with a Bruker SMART Apex diffractometer using Mo Kα radiation (λ=0.71073 Å) and graphite monochromator. Crystal data for **7a**: $C_{33}H_{42}Cl_6O_4S_4$, M_r=843.61, crystal dimensions 0.33×0.28×0.18 mm, orthorhombic, *Pnnm*, *a*=21.4233(12) Å, *b*=6.3455(4) Å, *c*=14.7914(8) Å, α=β=γ=90°, *V*=2010.8(2) Å^3, *Z*=2, ρ_{calcd}=1.393 g cm^{-3}, *F*(000)=876, μ=0.670 mm^{-1}, 2θ_{max}=26.00°, 15,275 measured reflections, 1948 independent reflections (R_{int}=0.0602) with $I\geq2\sigma$ (*I*), R_1=0.0572 ($I\geq2\sigma$ (*I*)) and 0.0765 (all data), wR_2=0.1415 ($I\geq2\sigma$ (*I*)) and 0.1514 (all data), GOF=1.023, 0.986, and −0.506 e Å^{-3} max. and min. residual electron density.

Crystal data for **7b**: $C_{33}H_{42}O_5S_4$, M_r=646.91, crystal dimensions 0.38×0.28×0.20 mm, orthorhombic, *Pbcn*, *a*=15.8500(7) Å, *b*=10.1413(4) Å, *c*=20.1608(9) Å, α=β=γ=90°, *V*=3240.6(2) Å^3, *Z*=4, ρ_{calcd}=1.326 g cm^{-3}, *F*(000)=1376, μ=0.333 mm^{-1}, 2θ_{max}=29.99°, 23,003 measured reflections, 4570 independent reflections (R_{int}=0.0165) with $I\geq2\sigma$ (*I*), R_1=0.0348 ($I\geq2\sigma$ (*I*)), and 0.0404 (all data), wR_2=0.0905 ($I\geq2\sigma$ (*I*)) and 0.0957 (all data), GOF=1.048, 0.458, and −0.230 e Å^{-3} max. and min. residual electron density.

Crystal data for **8**: $C_{28}H_{38}O_4S$, M_r=470.64, crystal dimensions 0.57×0.42×0.24 mm, tetragonal, *P4(3)2(1)2*, *a*=10.2539(2) Å, *b*=10.2539(2) Å, *c*=25.1993(10) Å, α=β=γ=90°, *V*=2649.52 Å^3, *Z*=4, ρ_{calcd}=1.180 g cm^{-3}, *F*(000)=1016, μ=0.152 mm^{-1}, 2θ_{max}=25.99°, 22,029 measured reflections, 2522 independent reflections (R_{int}=0.0351) with $I\geq2\sigma$ (*I*), R_1=0.0922 ($I\geq2\sigma$ (*I*)), and 0.0943 (all data), wR_2=0.2072 ($I\geq2\sigma$ (*I*)) and 0.2084 (all data), GOF=1.112, 0.280, and −0.289 e Å^{-3} max. and min. residual electron density.

Absorption corrections were made using the SADABS program.[26] The structures were solved by direct methods and refined on F^2 by full matrix least squares using SHELXTL.[27] All non-

hydrogen atoms were refined anisotropically. All H atoms in **7a**, **7b**, and **8** were placed in calculated positions and were refined in the riding model. CCDC-743592 (**7a**), 743593 (**7b**) and 765938 (**8**) contain the supplementary crystallographic data for this paper. These data can be obtained free of charge via www.ccdc.cam.ac.uk/conts/retrieving.html (or from the Cambridge Crystallographic Data Centre, 12 Union Road, Cambridge CB21EZ, UK; fax: (+44) 1223 336 033; or deposit@ccdc.cam.ac.uk).

Acknowledgements

We gratefully acknowledge the financial support of the Russian Foundation for Basic Research, grants 10-03-00788-a and 09-03-97034-r_povolzh'e_a and the Program for support of Leading Scientific Schools NSh-7065.2010.3. This work was made according to FSP "Scientific and scientific-pedagogical cadres of innovation Russia" for 2009–2013 years (GK-P839 from 25.05.2010).

Supplementary data

Supplementary data associated with this article can be found in the online version, at doi:10.1016/j.tet.2010.07.038. These data include MOL files and InChiKeys of the most important compounds described in this article.

References and notes

1. Perepichka, D. F.; Bryce, M. *Angew. Chem., Int. Ed.* **2005**, *44*, 5370–5373.
2. Bendikov, M.; Wudl, F.; Perepichka, D. *Chem. Rev.* **2004**, *104*, 4891–4945.
3. Bryce, M. R. *Adv. Mater.* **1999**, *11*, 11–23.
4. Gautier, N.; Dumur, F.; Lloveras, V.; Vidal-Gancedo, J.; Veciana, J.; Rovira, C.; Hudhomme, P. *Angew. Chem., Int. Ed.* **2003**, *42*, 2765–2768.
5. Dumur, F.; Gautier, N.; Gallego-Planas, N.; Sahin, Y.; Levillain, E.; Mercier, N.; Hudhomme, P.; Masino, M.; Girlando, A.; Lloveras, V.; Vidal-Gancedo, J.; Veciana, J.; Rovira, C. *J. Org. Chem.* **2004**, *69*, 2164–2177.
6. Abakumov, G. A.; Cherkasov, V. K.; Lobanov, A. V. *Dokl. AN SSSR* **1982**, *266*, 361–363.
7. Pierpont, C. G. *Coord. Chem. Rev.* **2001**, *219–221*, 415–433.
8. Sato, O.; Tao, J.; Zhang, Y.-Z. *Angew. Chem.* **2007**, *119*, 2200–2236; *Angew. Chem., Int. Ed.* **2007**, *46*, 2152–2187.
9. Narita, M.; Pittman, C. U. *Synthesis* **1976**, 489–514.
10. Yamada, N.; Furukawa, M.; Nishi, M.; Takata, T. *Chem. Lett.* **2002**, 454–455.
11. Takata, T.; Saeki, D.; Makita, Y.; Yamada, N.; Kihara, N. *Inorg. Chem.* **2003**, *42*, 3712–3714.
12. Breitzer, J. G.; Chou, J.-H.; Rauchfuss, T. B. *Inorg. Chem.* **1998**, *37*, 2080–2082.
13. Kuropatov, V. A.; Cherkasov, V. K.; Kurskii, Y. A.; Fukin, G. K.; Abakumova, L. G.; Abakumov, G. A. *Russ. Chem. Bull. Int. Ed.* **2006**, *55*, 708–711.
14. Hoskins, R. *J. Chem. Phys.* **1955**, *23*, 1975–1976.
15. Vinsow, G.; Fraenkel, G. K. *J. Chem. Phys.* **1961**, *34*, 1333–1344.
16. Muraev, V. A.; Abakumov, G. A.; Razuvaev, G. A. *Dokl. AN SSSR* **1974**, *217*, 212–215.
17. Belostotskaya, N. S.; Komissarova, N. L.; Dzhuaryan, E. V.; Ershov, V. V. *Bull. Acad. Sci. USSR, Div. Chem. Sci. Int. Ed.* **1973**, *22*, 1340–1341.
18. Rosokha, S. V.; Dibrov, S. M.; Rosokha, T. Y.; Kochi, J. K. *Photochem. Photobiol. Sci.* **2006**, *5*, 914–924.
19. Schultz, A. J.; Stucky, G. D.; Craven, R.; Schaffman, M. J.; Salamon, M. B. *J. Am. Chem. Soc.* **1976**, *98*, 5191–5197.
20. Abboud, K. A.; Clevenger, M. B.; Oliveira, G. F.; Talham, D. R. *J. Chem. Soc., Chem. Commun.* **1993**, 1560–1562.
21. Reichardt, C. *Solvents and Solvent Effects in Organic Chemistry*; VCH Verlagsgesellschaft mbh, D-6490: Weinheim, 1988.
22. Jigami, T.; Takimiya, K.; Otsubo, T. *J. Org. Chem.* **1998**, *63*, 8865–8872.
23. Prokof'ev, A. I.; Solodovnikov, S. P.; Belostotskaya, I. S.; Ershov, V. V. *Russ. Chem. Bull.* **1974**, *1*, 189–191.
24. Weissberger, A.; Proskauer, E. S.; Riddick, J. A.; Toops, E. E. *Organic Solvents. Physical Properties and Methods of Purification*; Interscience Publ.: New-York—London, 1955.
25. Garnov, V. A.; Nevodchikov, V. I.; Abakumov, G. A.; Cherkasov, V. K.; Abakumova, L. G.; Kurskii, Y. A. *Bull. Acad. Sci. USSR, Div. Chem. Sci. Int. Ed.* **1984**, *34*, 2589–2591.
26. Sheldrick, G. M. *SADABS v.2.01, Bruker/Siemens Area Detector Absorption Correction Program*; Bruker AXS: Madison, Wisconsin, USA, 1998a.
27. Sheldrick, G. M. *SHELXTL v. 6.12, Structure Determination Software Suite*; Bruker AXS: Madison, Wisconsin, USA, 2000.